

## A Chitosan Gold nanoparticles Molecularly Imprinted Polymer Ciprofloxacin Sensor

Sandeep G. Surya<sup>a‡</sup>, Shahjadi Khatoon<sup>b‡</sup>, AbdellatifAit Lahcen<sup>a</sup>, An T. H. Nguyen<sup>a</sup>, Boris B. Dzantiev<sup>c</sup>, Nazia Tarannum<sup>b\*</sup>, Khaled N Salama<sup>a\*</sup>

<sup>a</sup>Sensors lab, Advanced Membranes and Porous Materials Center, Computer, Electrical and Mathematical Science and Engineering Division, King Abdullah University of Science and Technology (KAUST), Saudi Arabia

<sup>b</sup>Department of Chemistry, Chaudhary Charan Singh University Meerut India 250004

<sup>c</sup>A.N. Bach Institute of Biochemistry, Research Centre of Biotechnology of the Russian Academy of Sciences, Moscow, Russia

Corresponding author: [naz1012@gmail.com](mailto:naz1012@gmail.com), [Khaled.salama@kaust.edu.sa](mailto:Khaled.salama@kaust.edu.sa)

### Supplementary material:

5mL of each prepared solution of MIP, NIP and adduct, were dried in petri dish using incubator at 50°C The dried adduct was washed by the solvent methanol and acetic acid (9:1) four times and dried to obtain MIP film [1].

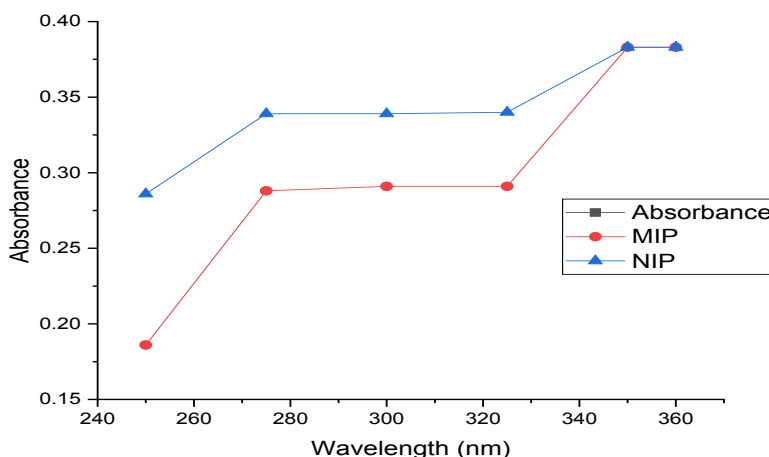


**Fig S1:** Comparative graph b/w MIP and NIP (Abs vs Wavelength)

Prepare the ciprofloxacin solution (50mg in 20 mL D.W) for each adduct ,MIP and NIP then 50mg of the dried MIP, NIP and adduct were dipped in ciprofloxacin solution for 10 min (optimized time) and now added MIP and NIP film in the two solution of CIP and observed UV-vis. It was found that minimum absorbance was of the solution in which MIP film was dipped due to the presence of binding cavities whereas, the concentration of CIP was high for the solution in which NIP was dipped.

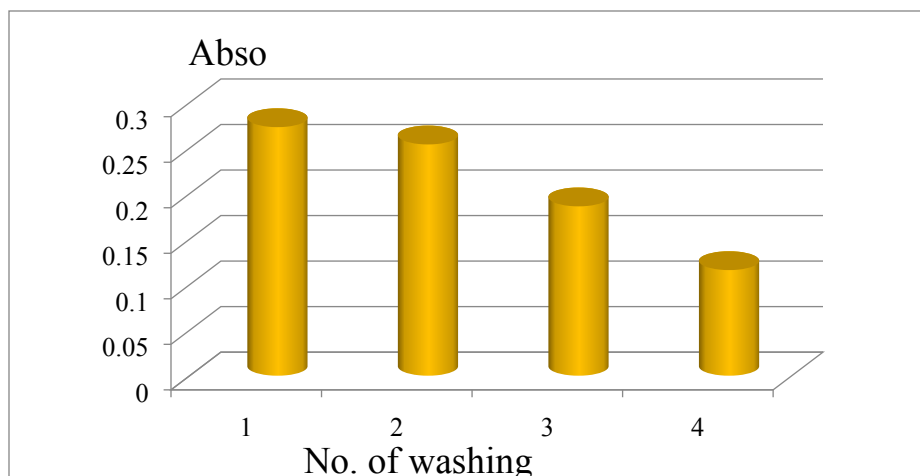
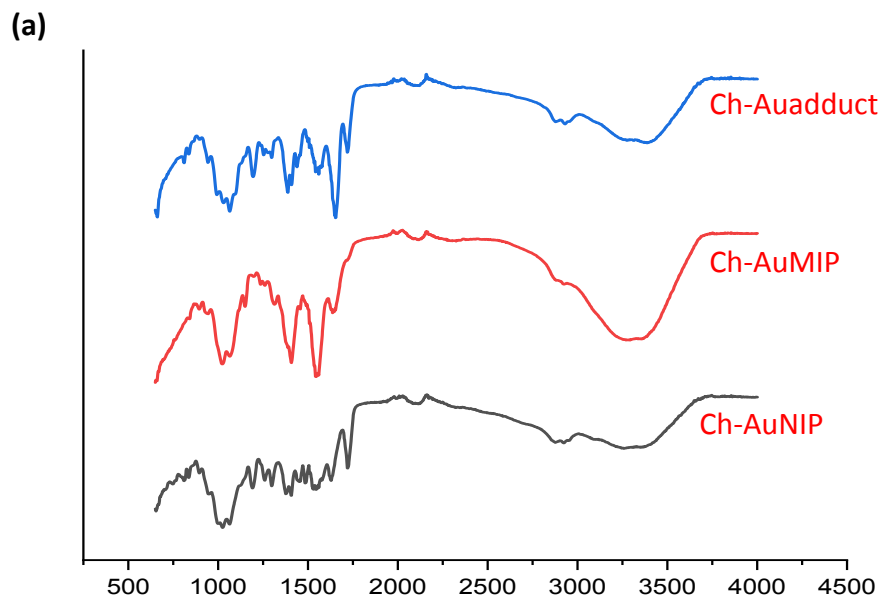
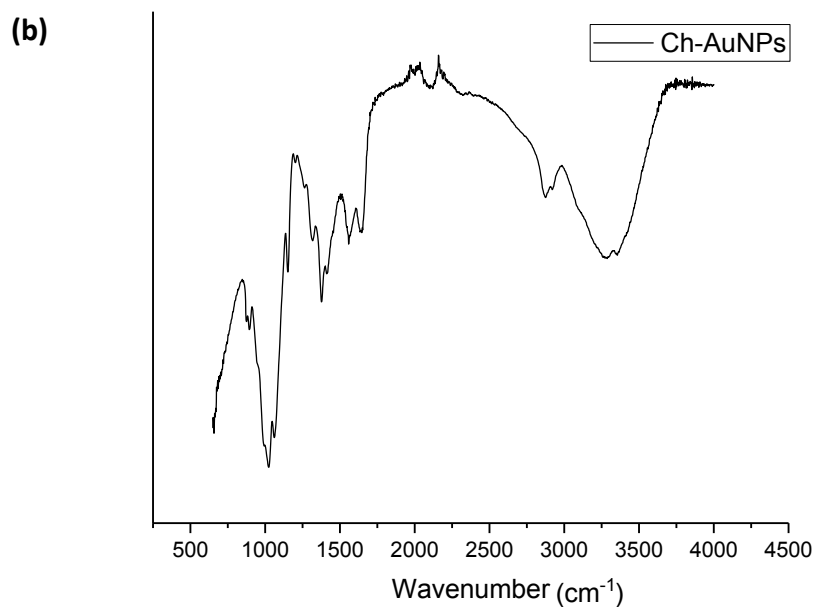


Fig S2: Graph between Abs vs no of washing

We also obtained the UV-Vis of the eluted solvent after washing four times. It is found that the concentration of first washing solvent is higher than second third and fourth at the wavelength range 270nm. It means concentration of solvent decreases by increasing number of washes.





**Fig S3: (a)** Comparative study of FTIR of Adduct, Ch-AuMIP and Ch-AuNIP (b) FTIR of Ch-AuNP

**Table S1 Comparison of FT-IR spectra of NIP, MIP, and Adduct**

Wavenumber ( $\text{cm}^{-1}$ ) NIP	Wavenumber ( $\text{cm}^{-1}$ ) MIP	Wavenumber ( $\text{cm}^{-1}$ ) Adduct	Absorption band assignment
894	889	833	-CH wagging
1019	1027	1027	C-OH, C-O-C stretching
-	-	1064 strong	C-F stretching
1196	1152	1193	C=O asymmetric vibration
1303	1312	1312	C-N stretching
1375	1398	1385	-CH <sub>2</sub> stretching
1532	1560	1552	C=O group of amide
1630 weak	1647 weak	1654 strong	-NH bending
1720	1722 weak	1722	C=O(group of acid) stretching
2926	2917	2917	-C-H stretching
3338	3351	3387 broad	-NH , -OH stretching

The given peaks shift toward the lower wavenumber in case of Ch-AuNP as compared to chitosan is due to electrostatic interaction between polymer and NPs.

**Table S2 FT-IR of the Ch-AuNP spectra**

Ch-AuNP, peak(cm <sup>-1</sup> )	Chitosan, peak(cm <sup>-1</sup> )	Peak assignment with reference
1637	1628	Amide group[1]
1549	1542	Free amine group[1]
1370	1379	C-C stretching of the glucosamine group of chitosan[2]

[1] A. Futyra, M. Liskiewicz, V. Sebastian, S. Irusta, M. Arruebo, G. Stochel, A. Kyzioł, Applied Material & Interfaces, 2015, 7, 1087–1099.

[2] C. O. Mohan, S. Gunasekaran, C. N. Ravishankar, NPJ Science of Food, 2019, 3, 2.

Composition of Ch-AuNP = Chitosan, AuNP.

Composition of Ch-AuNIP = Chitosan, AuNP, Methacrylic acid (MAA), Ethylene glycol dimethacrylic acid (EGDMA), Azobisisobutyronitrile (AIBN)

Composition of Ch-AuAdduct = Chitosan, AuNP, Methacrylic acid (MAA), Ethylene glycol dimethacrylic acid (EGDMA), Azobisisobutyronitrile (AIBN), Ciprofloxacin

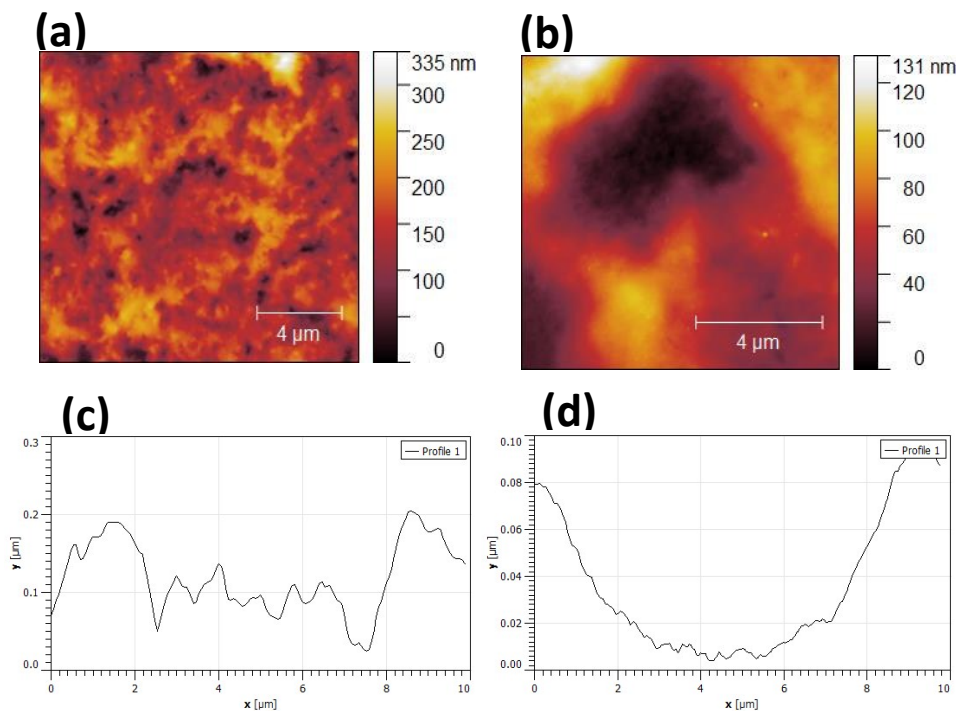


**Fig. S4:** AFM images of both the MIP and NIP in 2D profiles where (a) and (b) corresponds to Ch-Au-MIP and Ch-Au-NIP and the corresponding height profiles in(c) & (d) height profiles of MIP and NIP

2D AFM images of MIPs show many small pores in the range of hundreds of nm range spread in a sporadic manner all over the surface. The depth profiles indicate a range of (150 nm to 200 nm) throughout. Whereas, in the case of NIPs, we observed shallow pinholes with depths of approximately 80 nm and they are very few in number. Hence, MIP provides more scope for the mechanical binding of CIP due to suitable pores and the NIP based sensor with cracks has a different effect due to which we see the changes in response.

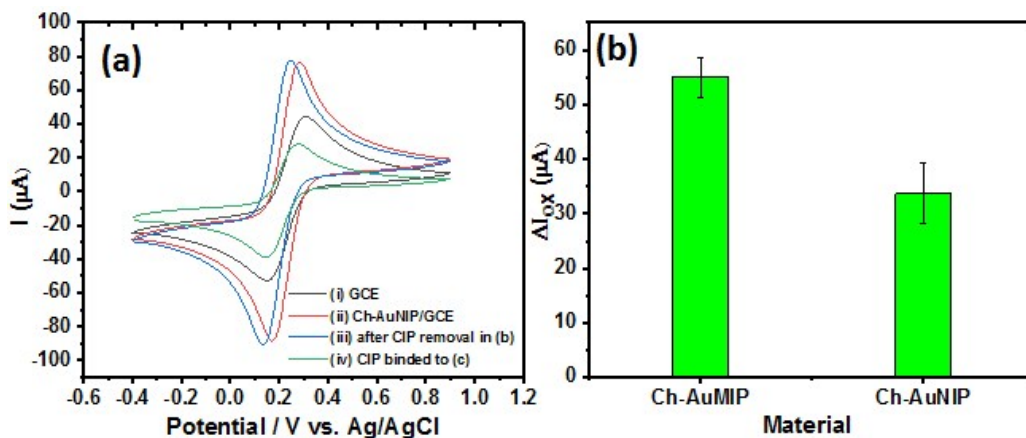


**Fig. S5:**(a) Cyclic voltammograms of different electrodeconfigurations in 5 mM  $[\text{Fe}(\text{CN})_6]^{3-/4-}$  containing 0.1 M KCl (i) GCE, (ii) Ch-AuNIP/GCE (iii) Ch-AuMIP/GCE after removal of CIP with MeOH/AAc (iv) Ch-AuMIP/GCE after binding CIP (b) Ch-AuMIP/GCE and Ch-AuNIP/GCE responses towards 10-5M of CIP in a 5 mM solution of Fericyanide containing 0.1M KCl

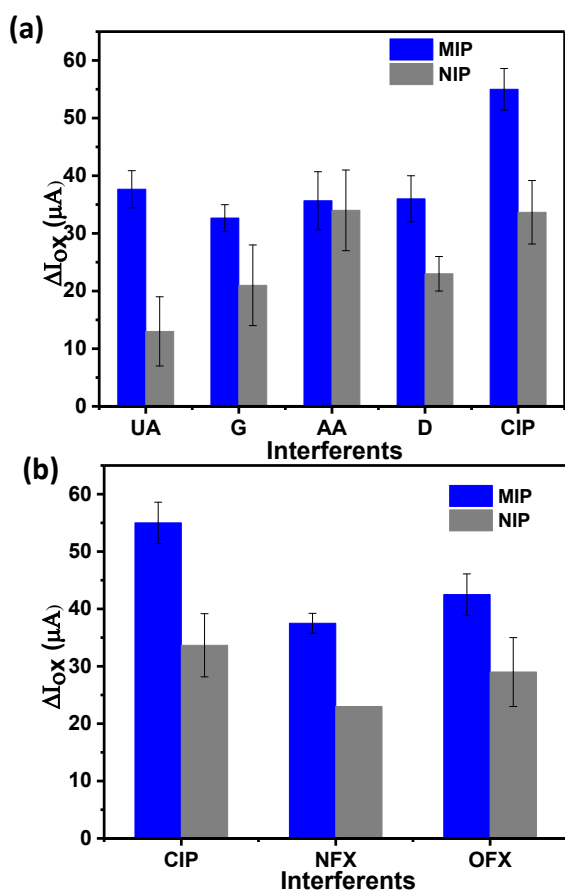


**Fig. S6:**(a) Response of the Ch-AuMIP and Ch-AuNIP sensing system in the presence of 10 $\mu$ M of Ciprofloxacin (CIP), Uric Acid (UA), Glucose (Glu), Ascorbic Acid (AA) and Dopamine(DA) (b) Response of the developed sensing strategy towards CIP and other similar structure analogue molecules of Norfloxacin (NFX) and Ofloxacin (OFX).

**Table S3: ANOVA calculation Table:**

Anova Single Factor							
SUMMARY							
Groups	Count	Sum	Average	Variance			
Column 1	3	28.18	9.393333	0.144633			
Column 2	3	29.94	9.98	0.0004			
Column 3	3	29.97	9.99	0.5184			
Column 4	3	32.4	10.8	0.2025			
Column 5	3	31.8	10.6	0.09			
ANOVA							
Source of Variation	SS	df	MS	F	P-value	F crit	

Between Groups	3.756027	4	0.939007	4.911465	0.018837	3.47805
Within Groups	1.911867	10	0.191187			
Total	5.667893	14				